MoS_2 modified Screen Printed Carbon Electrode based Flexible Electrochemical sensor for Detection of Copper ions in water

Deepan Kumar Neethipathi, Ajay Beniwal, Adrian Bass, Marian Scott, Ravinder Dahiya, *Fellow IEEE*

***Abstract*—Heavy metal ions such as Cu^{2+} are harmful to the environment and our health. Such ions are typically measured using glassy carbon electrode (GCE) based electrochemical sensors developed on rigid substrates. However, several emerging applications require such sensors on flexible, and even disposable, substrates. Herein, we present a MoS_2-modified screen-printed carbon electrode (SPCE) based flexible electrochemical sensor for the detection of copper ions in the water. The sensor exhibits excellent response with a limit of detection (LOD) of 5.43 μM for Cu ions in the range of 5 μM to 5 mM. The developed sensor is compared with MoS_2-modified conventional glassy carbon electrode using electrochemical impedance spectroscopy (EIS). The comparative studies show better linearity (R^2 value ~ 0.99) for SPCE-based sensor and underlines how easily they can detect Cu ions. The interference study, i.e., detection of copper ions in presence of other heavy metal ion-based analytes, also show the excellent response of SPCE based flexible electrochemical sensor – thus demonstrating their practical application is the detection of Cu in water.**

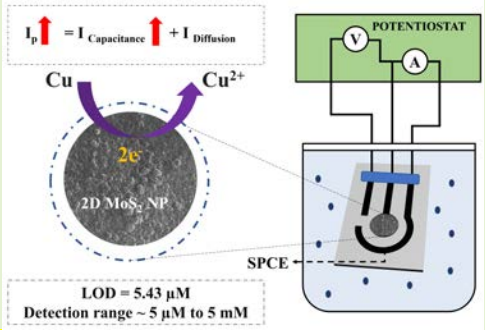

***Index Terms*—Copper detection, electrochemical sensor, flexible sensor, heavy metal, MoS_2, screen-printing.**

I. Introduction

PRESENCE of heavy metals in water bodies is one of the major global concerns that adversely affect the ecosystem and human health. This is because heavy metal ions are non-biodegradable, can create toxicity, and have longer half-life time, etc. [1, 2] As a result, the research on sensors for heavy metal ion (HMI) detection has attracted considerable attention. Among various HMIs, Copper is most readily found in water. It comes through multiple sources such as paints [3], pesticides [4], electronics [5], functional inks [6], and semiconductor industries [7]. The accumulation of unbounded copper ions acts as a chemical pollutant in underground water supplies [8]. The maximum containment level (MCL) of copper is 1.3 mg/L and 2 to 4 mg per day as an essential as the dietary requirement for the human body [9, 10]. Severe health issues such as Wilson disease, gastrointestinal disturbances, and liver damage are caused due to the higher consumption of copper in drinking water [11, 12].

Typically, Copper is detected in field using high spectroscopic techniques such as colorimetric [13, 14], inductively coupled plasma mass spectroscopy[15], instrumental neutron activation analysis [16, 17], atomic absorption spectroscopy [18, 19], and fluorescence spectrometry [20, 21] etc. These methods provide excellent sensitivity for the detection of copper ions in water (in the femtomolar range) but also require frequent maintenance and skills to operate. Moreover, these instruments are bulky and lack portability. The electrochemical sensors can provide an attractive alternative for the detection of copper as they typically exhibit favorable parameters such as desirable selectivity, quicker response, and operable sensitivity. Further, they can be self-powered and fabricated on various types of flexible and disposable substrates [22-25]. Due to simple and cost efficient fabrication processes, many low-cost printed biosensors have been reported for the detection of copper ions [26-28] and among the various attributes they offer the

This work was supported by European Commission through the Innovative Training Network AQUASENSE (H2020-MSCA-ITN-2018-813680). An earlier version of this paper was presented at the 2022 IEEE International Conference on Flexible and Printable Sensors and Systems (FLEPS) (DOI: 10.1109/FLEPS53764.2022.9781564). (Corresponding author: Ravinder Dahiya).

D. K. Neethipathi and A. Beniwal are with School of Engineering, University of Glasgow, Glasgow G12 8QQ, U.K.

A. Bass is with School of Geography and Earth Science, University of Glasgow, Main Building, Glasgow G12 8QQ, U.K.

M. Scott is with School of Mathematics and Statistics, University of Glasgow, University Place, Glasgow G12 8SQ, U.K.

R. Dahiya is with Bendable Electronics and Sustainable Technologies (BEST) Group, Electrical and Computer Engineering Department, Northeastern University, Boston, MA 02115, USA. (email – r.dahiya@northeastern.edu).

flexibility is distinct as it allows them to conform to curved surfaces and hence useful for several practical applications [29-31].

Herein, we present a flexible electrochemical sensor comprising of molybdenum disulfide (MoS_2) sensing layer, on top of the screen-printed carbon-electrode. The 2-Dimensional MoS_2 is an excellent transition metal dichalcogenide (TMDs) material which offers many advantageous traits such as good chemical stability, better biocompatibility, provide a larger surface area, and offers excellent electrocatalytic properties. Hence, it has gained considerable attention for sensor applications in areas such as pharmaceutical, food, medical and environmental containment monitoring [32-35]. Conventional electrochemical sensors are typically fabricated on rigid substrates (e.g., glass). Here we chose to fabricate the sensors on flexible substrate as their flexibility helps them to operate in harsh field conditions without any breakage [36, 37]. These flexible sensors can be miniaturized to improve the portability and their fabrication by printing could also ensure the resource efficient manufacturing[38]. However, the electrochemical sensor on rigid substrates can be superior in terms of sensitivity and performance[39].

This paper also extends our initial work presented at IEEE International Conference on Flexible and Printable Sensors and Systems (FLEPS) 2022 [40]. In this extended work, we have analyzed the electrochemical behavior of both the modified glassy carbon electrode (GCE) and the screen-printed carbon electrode (SPCE) using electrochemical impedance spectroscopy (EIS) techniques. The comparative impedance spectroscopy analysis between the performance of conventional GCE based rigid sensors and the screen-printed carbon electrode based flexible sensors shows that the capacitive behavior of MoS_2 based printed carbon-based sensor helps in finer detection between linear dynamic range i.e., providing better change of peak current value (ΔIp) between different concentrations of copper detection. The cyclic voltammetry (CV) and differential pulse voltammetry (DPV) techniques are also used for the detection of copper ions in water using MoS_2 nanomaterials modified glassy carbon and screen-printed carbon-based electrode and their performance is compared. In addition, the performance of MoS_2 modified SPCE based electrochemical sensor is studied with other similar interfering heavy metal ions.

This paper is organized as follows: the materials and methods used, the fabrication of the screen-printed sensor, and the experimental setup are described in Section II. The material synthesis technique, their characterization, electrochemical performance for the copper detection, EIS study results, and interference studies are given in Section III. Finally, the key outcomes are summarized in Section IV.

II. MATERIALS AND METHODS

A. Materials

Commercially available sodium molybdate, thiourea, copper chloride, dimethylformamide (DMF), Teflon, terpineol, and phosphate buffer saline tablets were purchased from Merck. These chemicals were used without any further modification. The conductive carbon paste and the grey dielectric paste used here (for screen-printed electrodes) were obtained from Sun Chemical. A glassy carbon electrode (GCE) was purchased from Alvotek ltd.

B. Synthesis of 2D-MoS_2 Nanoparticles

The precursor solution was made by mixing sodium molybdate and thiourea in the mole ratio of 1:4 (0.020 moles to 0.080 moles) along with deionized water. The mixture is stirred well for 60 minutes at room temperature. The above mixture was transferred to a 100 mL Teflon-lined stainless-steel autoclave, and it was left inside a heating oven for a day at 220ºC. The molybdenum disulfide (MoS_2) nanomaterials were obtained as a black precipitate from the above mixture using hydrothermal synthesis. For further purification, the obtained black precipitate was washed multiple times with water and IPA using a centrifuge and left for drying at 60ºC [41]. The MoS_2 nanoparticle was then dispersed in 20 ml of DMF using probe ultrasonication for 6 hrs to obtain the solution needed for sensor fabrication. The synthesis process is illustrated in Fig. 1.

C. Sensor fabrication via screen printing

A schematic representation of the screen printing of thick film electrodes is shown in Fig. 2. Screen Stencil Printer C920 from AUREL Automation is used for the screen printing. Before screen-printing, the commercially available carbon paste was blended well with IPA and terpineol to obtain a paste with a viscosity suitable for printing. For the three-electrode system, all electrodes (i.e., working electrode (WE), counter electrode (CE), and reference electrodes (RE)) were screen printed onto a flexible PVC substrate using the blended carbon paste ink. Here, the diameter of the circular working electrode is 0.5 cm. Then multiple layers (20) were printed to obtain a thick electrode layer [42]. The printed electrodes were dried after each layer of printing to avoid spreading or smudging of already printed electrodes. This was achieved by placing the sample in an oven at 70 ºC. The same conductive carbon paste was used to make the wire connections. The dried interconnection was covered with a thick layer of grey dielectric

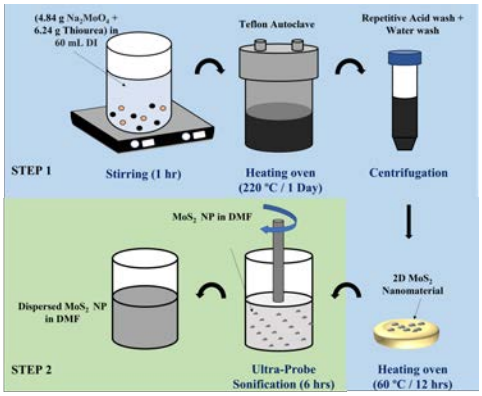

Fig. 1. Step (1) Preparation of 2D MoS_2 nanomaterial from sodium molybdate and thiourea; Step (2) Preparation of MoS_2 ink by dispersing MoS_2 in DMF solution using ultra-probe sonification.

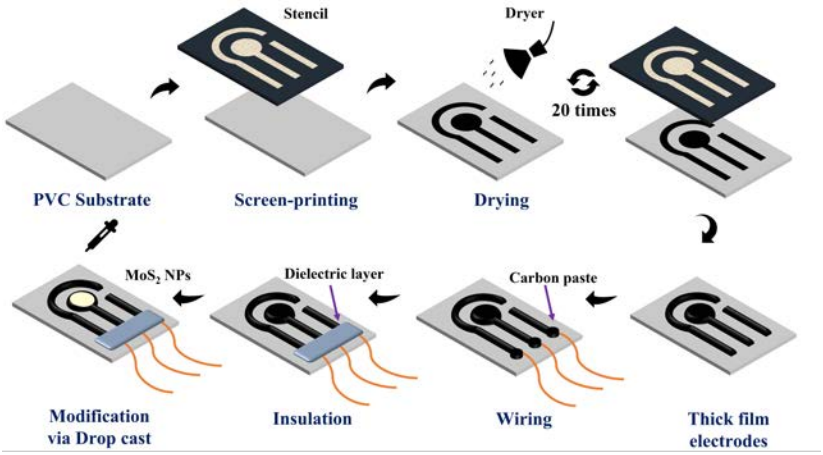

Fig. 2. The manufacturing procedure of bulk electrodes for MoS_2 modified screen printed sensor.

paste to avoid short-circuiting the electrodes.

D. Modification of GCE and SPCE using drop casting

For GCE and SPCE modification, we used 20 µl of the dispersed MoS_2 nanoparticle in DMF solution, and drop casted over the circular working region using a micropipette. Following this the sensor was kept in the oven at 65ºC for 45 mins. Multiple layers of MoS_2 were stacked on top of each other layers by successive drop casting, with 5 µl of solution every time with intermediate drying at oven. Here, the other electrodes (Counter, Reference) are unmodified.

E. Electrochemical measurements

The cyclic voltammetry (CV), differential pulse voltammetry (DPV), and electrochemical impedance spectroscopy (EIS) were performed using an electrochemical workstation (Metrohm Autolab (PGSTAT302N)) to study the electrochemical behavior of the fabricated sensor. To perform these studies, a neutral ionic solution of constant PH 7 was made, by dissolving 1 tablet of PBS in 500 mL of deionized (DI) water. The prepared PBS solution of 0.1 M was used as the electrolyte during electrochemical experiments. To prepare the analyte stock and other interference solutions, concentrations of 1 mM and 100 mM were prepared by adding deionized water along with copper, iron, cobalt, zinc, and nickel. For performing the voltametric techniques, these solutions were diluted and further added along with 9 ml of PBS solution to achieve various concentrations of the analyte solutions (i.e., 1 µM to 1 mM).

III. RESULTS AND DISCUSSION

A. Material Characterisation

Fig. 3(a) shows the X-Ray diffraction (XRD) patterns that were acquired for the resultant product. Here the red line indicates the XRD pattern for the synthesized powder and the peaks obtained at 14.17º, 33.45º, 39.5º, 49.17º, 58.84º and 69.43º can be indexed easily towards the lattice points (002), (100), (103), (105), (110) and (201), respectively, of 2-H MoS_2 the hexagonal phase of 2-H MoS_2 concerning ICDD card no: 37-1492[43]. Similarly, the XRD pattern for the printed SPCE is shown as the blue plot. The scanning electron microscopy (SEM) images, in Fig. 3 (b-d), were taken for the synthesized MoS_2 powder, unmodified SPCE, and MoS_2 modified over SPCE respectively, to understand their surface morphology. The SEM image of synthesized MoS_2 nanoparticle powder indicated an agglomerated cluster of spherical nanoparticles, whereas the SEM image of the SPCE shows a smooth layer of a well-homogenous carbon ink surface. After drop-casting the well-dispersed MoS_2 nanoparticle solution over the SPCE, a high roughness surface along with cracks was seen in the SEM image of the modified SPCE. The presence of MoS_2

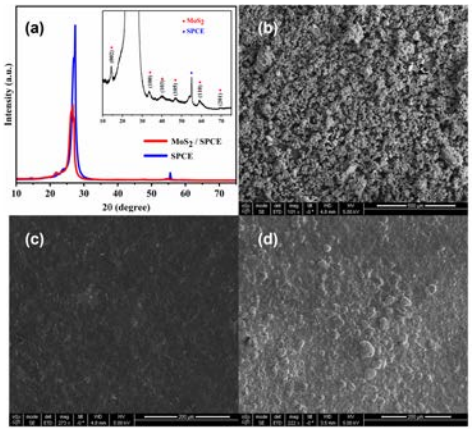

Fig. 3. (a) shows the XRD Pattern for MoS_2 powder and MoS_2 coated SPCE layer; SEM images of (b) MoS_2 powder (c) SPCE, (d) MoS_2 modified SPCE.

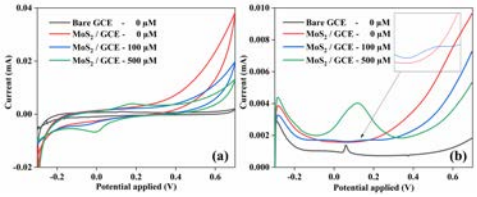

Fig. 4. (a, b) CV and DPV responses for MoS_2 coated GCE layer in the presence of 0, 100, 500 μM Cu^{2+} ions in 0.1M PBS respectively.

nanoparticles that were modified over SPCE was confirmed through the SEM images.

B. Detection of copper ions by MoS_2-coated GCE

The 3-electrode system used here includes the MoS_2 modified GCE as the working electrode, platinum coil as the counter electrode, and Ag/AgCl electrode as the reference electrode. In Fig. 4(a, b), both CV and DPV responses are displayed for the bare and MoS_2 modified GCE in the absence and presence of 100 µM, and 500 µM. Here, the difference between the peak current value for the detection of Cu^{2+} ion between the concentrations of 100 µM and 500 µM is 0.00228 mA.

C. Detection of copper ions by MoS_2 modified screen-printed electrode-based sensor

Fig. 5(a) displays the fabricated SPCE-based sensor after MoS_2 modification. Fig. 5(b) helps us to understand the electrochemical detection of copper ions using the MoS_2 modified SPCE-based sensor. Here, the black and red lines represent the CV curve for both bare SPCE and MoS_2 modified SPCE in the blank 0.1 M PBS solution. The blue line shows the CV curve in the presence of 100 µM of copper ions in PBS solution, where both the oxidation and reduction peaks are visible at 0.2 V and -0.01 V. Thus, it helps us to understand the occurrence of the redox reaction of copper, which can be further detected by the MoS_2-coated SPCE layer. Then the DPV curve is obtained in Fig. 5(c), where the peak anodic peak in the blank line is the result of modification caused by MoS_2, which is used to detect the concentration of the analyte. Here the obtained red line for the same range from -0.3 V to 0.8 V at the step potential at 5 mV/pulse confirms the rise in the peak anodic current. Further, there is a slight shift in the peak voltage from 0.2 V to -0.01 V. The addition of 100 µM Cu analyte ions to the blank solution causes the oxidation of Cu ions and thus, a slight change in the anodic peak was observed.

D. Concentration studies

For the concentration studies, the cyclic voltammetry responses were obtained in the range of -0.3 V to 0.8 V, and the scan speed of 50 mV/s with varying concentrations of copper ions from 1 µM to 1000 µM in 0.1 M PBS as displayed in Fig. 5(d). The oxidation peaks for such varying concentrations i.e., 1 µM to 1000 µM are observed at 0.16 V to 0.19 V, and their corresponding reduction peaks are observed at 0.01 V to -0.03 V. The differential curve in Fig. 5(e) shows anodic current peaks shifting in the region of 0.04 V to 0.06 V when the analyte concentrations were varied in 0.1 M PBS solution. Here, the difference between the peak current value for concentrations of 100 µM and 500 µM is found to be 0.00904 mA, which is 4 times higher than the change seen in the modified GCE. To understand the electrochemical behaviour of the fabricated sensor, the CV and DPV response for higher concentrations i.e., 2 mM to 10 mM were obtained and shown in Fig. 5 (f, g). Based on the DPV curve response, the anodic peak current rises until 5 mM in the region of 0.07 V. The shape of the DPV peak curve obtained for 10 mM expands drastically over the region of -0.3 V to 0.1 V with a negative peak shift at -0.05 V, making it undetectable and out of the detection range. To find their linearity, the Cu concentrations between 5 µM to 1 mM are plotted against their respective DPV peak current value as shown in Fig. 5(h). Two linear detections were found over 5 µM to 1000 µM.

An initial sharp rise was found over the first linear range i.e., between 5 to 50 µM with high linearity (R^2 value - 0.99972). Their linear regression equation is expressed as follows:

$$Ip = 1.01278E\text{-}4*(Conc.Cu^{2+}) + 0.04897$$
$$R^2 = 0.99972 \quad (1)$$

This sharp rise in peak current between 5 µM to 50 µM indicates that the diffusion of loosened valence electrons caused by the oxidation of copper has plenty of electrocatalytic edge sites available on the surface of 2D MoS_2. The second linear range found over the higher concentrations i.e., 100 µM to 1000 µM shows the linearity of R^2 value 0.98605, and it was expressed by the linear regression expression as follows:

$$Ip = 1.74614E\text{-}5*(Conc.Cu^{2+}) + 0.05423$$
$$R^2 = 0.98605 \quad (2)$$

The second linear rise for the increasing peak current observed in the region over 100 µM to 1000 µM, can be explained by the partial blockage of active sites by the electrocatalytic edge sites after oxidation of a certain threshold concentration (100 µM in this case). Due to the deposition of oxidized copper ions i.e., cupric ions over the electrocatalytic edge sites of the MoS_2 sensing layer, the diffusion of loosened valence electrons is likely to have lesser active sites for further diffusion[44]. During the reduction phase, these deposited Cu^{2+} ions reduce to Cu ions, and thus the deposition onto the sensing layer is reversed. The slope found in both linear ranges is close to 0.05 which indicates that the increase in the concentration of Cu ion is directly proportional to the increase in peak current. Here, the limit of detection (LOD) was found to be 5.43 µM and the limit of quantification (LOQ) was 16.46 µM.

E. Effect of scan rate

To understand the sensing mechanism, we also obtained the CV scans at various scan speeds between 10 to 700 mV/s, as shown in Fig. 6(a). In this study, 100 µM copper ions were present in 0.1 M PBS solution. From the scan speed time and their recognizable peak presence, we obtained the optimized scan rate for the detection of analyte solution as 10 mV/s to 200 mV/s. The oxidation peak current value for each CV scan is

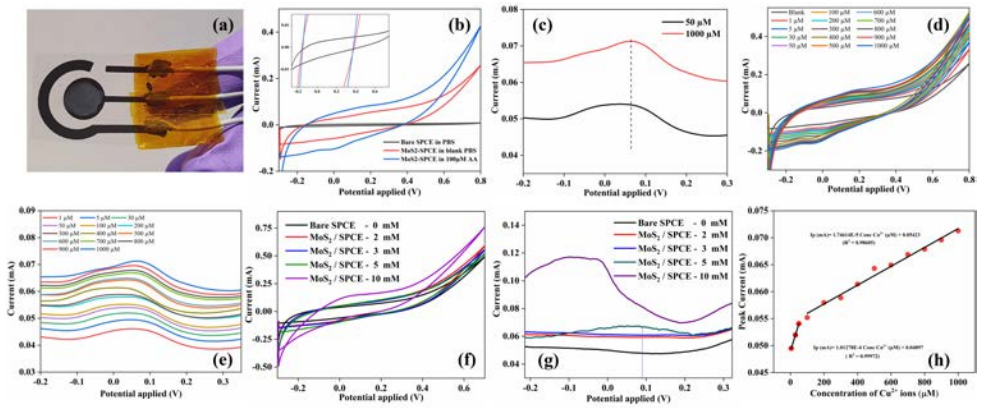

Fig. 5. (a) A photograph of the fabricated sensor. (b) CV curves of bare SPCE, MoS_2/SPCE in PBS solution & MoS_2/SPCE in 100 μM of copper ions in PBS solution. (c) DPV response curve for MoS_2/SPCE in the presence of 100 μM to 1000 μM of copper ions in PBS. (d, e) CV and DPV responses for 1 μM to 1000 μM of copper analyte in PBS solution. (f, g) CV and DPV responses for 2 mM to 10 mM of copper analyte in PBS solution. (h) Peak current (Ip) vs copper concentration between 1 μM to 1000 μM.

plotted against their corresponding scan rate in Fig. 6 (b) and the R^2 value is 0.8. The corresponding varying scan rate is plotted in Fig. 6 (c) against the square root of the oxidation peak value (Ip) and the R^2 value for their regression line is found to be 0.96. Thus, the regression line obtained from the plotted graph i.e., the square root of scan rate vs peak current value (Ip) is more linear than the regression line obtained from the plot of scan rate vs peak current value (Ip). These studies help us to understand that the sensing of analyte species is a more diffusion-controlled process than absorption-controlled. The logarithm of the oxidation peak current value is plotted against the logarithm of the scan rate in Fig. 6 (d) and the slope of their regression line is found to be 0.42848, which is close to the ideal diffusion-controlled process i.e., 0.5[45].

F. Interference Studies

The interference studies were carried out too and, in this regard, the CV and DPV responses are shown in Fig. 7 (a, b) for the electrochemical detection of the targeted analyte species i.e., 100 µM Cu^{2+} ions in the presence of other similar heavy metal ions such as nickel, zinc, cobalt, and iron. The CV and DPV responses of the interaction between the above similar analyte species are shown in the Fig. S1, S2, S3, and S4 of the supporting information, which was obtained by adding different HMIs (with concentrations such as 50 µM and 100 µM) to 100 µM Cu analyte ions in a 0.1 M PBS solution. From the interference study, it may be noted that the addition of Fe^{2+} majorly influences the response for the copper ion, as the peak shift in anodic DPV current was observed while Fe^{2+} ions were added.

G. Comparison of GCE and SPCEs

To compare the response SPCE with respect to GCEs, we obtained the Nyquist plots both in the absence and presence of 100 µM copper ions, as shown in Fig. 8 (a). Here, we used bare GCE with Ag/AgCl and platinum coil to run EIS measurements in the absence and presence of 100 µM Cu ions in 0.1 M PBS solution. In both cases, the absence of a semicircle at the high-frequency zone indicates that there is no formation of a double-layer region. This represents characteristics similar to a typical supercapacitor[46, 47]. This is due to the high conductivity and low charge transfer resistance of glassy carbon. However, at the lower frequency zone, this bare electrode shows the behaviour of a constant phase element (CPE) with a constant phase difference angle (θ) of 62º without copper ions and 84º with copper ions (n = 0.688 & 0.933). Here, the bare GCE shows imperfect capacitive behaviour with the addition of copper ions as the deviating angle stays closer to the ideal capacitor behaviour i.e., = 90º[48]. However, the series resistance of this bare electrode is almost constant at around 108 ohms in the presence and absence of Cu ions, indicating that there is no significant change in electrode to the electrolyte interaction in both cases. Fig. 8 (b) shows the Nyquist plot via EIS

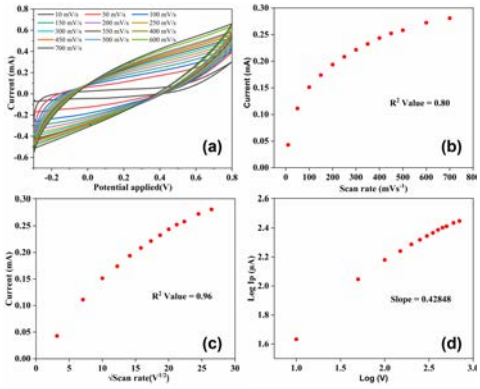

Fig. 6. (a) CV response curves for 100 μM of Cu^{2+} ions in PBS with scan rates of 10 to 700 mV/s; (b) I_P versus scan rate; (c) I_P versus √scan rate; (d) Log of I_P versus Log of scan rate.

Deleted: Figure
Deleted: detecting
Deleted: a different
Deleted:

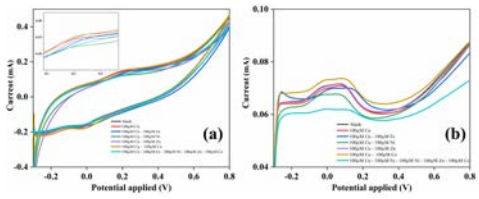

Fig. 7. (a) CV responses for the detection of 100 μM Cu ions, along with other heavy metal ions; (b) DPV responses for the detection of 100 μM Cu ions, along with other heavy metal ions.

measurements for the MoS_2 modified GCE, both in the absence and presence of Cu ions. Here, in the absence of Cu ions, a semicircle is not seen in the high-frequency region and the plot resembles a CPE at a lower frequency which is possibly due to the roughness at the surface of the electrode ($\theta = 41^o$). However, the presence of a partial semicircle in the higher frequency region could be due to a combination of electrode resistance and charge transfer resistance at the surface interface (double layer formation), thus acting as a CPE and followed by Warburg impedance ($\theta = 44^o$). As shown in Fig. 8 (c), the initial electrode resistance for the bare and modified GCE is calculated to be around 111.47 ohms to 113.5 ohms in the absence and presence of copper ions, respectively (fitted graph are shown in Fig S5 in supporting information).

Fig. 8 (d) shows the Nyquist plot for bare SPCE electrode, obtained from the EIS measurements in the absence and presence of the analyte solution i.e., 100 µM Copper ions. The bare SPCE shows similar CPE behavior at lower frequencies and no formation of double layer region (charge transfer resistance) due to its high conductivity. Here the constant phase (n) value was found to be 0.877 and 0.811 with the phase difference angle of 79º & 73º in the absence and presence of Cu ions respectively. Comparing the constant phase of these bare electrodes, it is noted that the capacitive impedance builds in MoS_2 modified GCE in the presence of analyte solution while the capacitive impedance drops in the case of SPCE. Fig. 8 (e) shows the Nyquist plot for the MoS_2 modified SPCE. For the absence and presence of analyte solution, a semicircle is formed at a higher frequency due to the double layer region, and CPE (n = 0.633 & 0.688 respectively) is seen in the lower frequencies. The electrode and electrolyte resistances for the bare and modified SPCEs are shown in Fig. 8 (f). The internal resistance due to both electrode and electrolyte for MoS_2 modified GCE and SPCE is found to be around 328.28 ohms and 370.27 ohms respectively. Their respective electrode resistances were measured from the fitted graphs as 279.57 ohms and 280.12 ohms respectively. Fig. S6 in the supporting section contains the Nyquist plot for all electrodes in both the absence and presence of 100 µM Copper ions. Fig. S7 in the supporting section includes the Bodes plot and Fig. S8 shows the Frequency vs. Impedance plots for all the above cases.

From above, it can be concluded that the modified GCE shows Warburg impedance which is the characteristic of an excellent diffusion-controlled process. And in the case of modified SPCEs, even if there is a slight tendency towards CPE characteristics (n = 0.633 & 0.688). This could be a result of both the capacitive nature of SPCE and ion diffusion. Further, the response current is the resultant of both surface-controlled and diffusion-controlled currents[49].

$$I_p = I_{capacitance} + I_{diffusion} \quad (3)$$

The overall peak current change observed in the modified

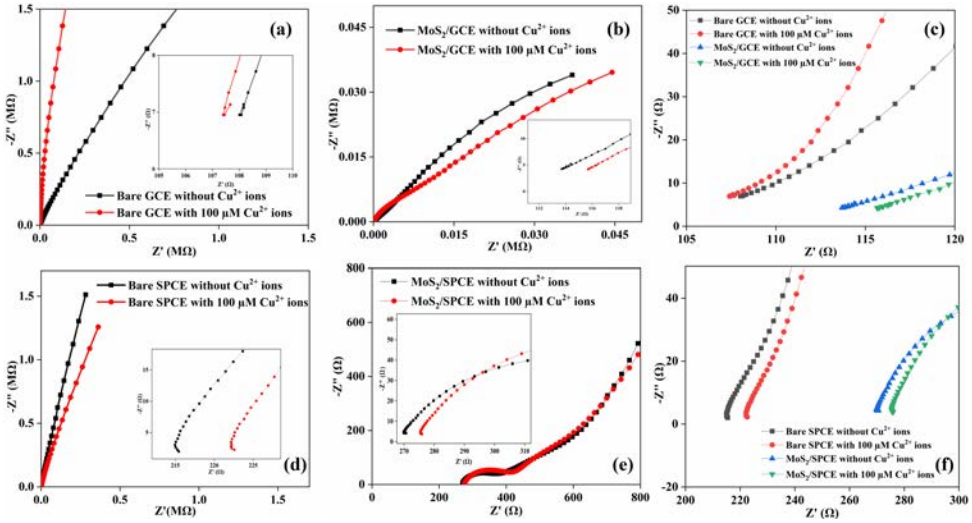

Fig. 8. (a, b) Nyquist plot for the bare GCE and bare SPCE electrodes in the absence and presence of 100 μM copper ions respectively; (c) Nyquist plot for both bare GCE and bare SPCE in the high-frequency region; (d, e) Nyquist plot for the MoS_2 modified GCE and MoS_2 modified SPCE electrodes in the absence and presence of 100 μM copper ions respectively; (f) Nyquist plot for both the MoS_2 modified GCE and MoS_2 modified SPCE in the high-frequency region.

Deleted: Figure

Deleted:

SPCE at different concentrations is higher than that observed for modified GCE. The high charge transfer resistance and the internal capacitance behavior of MoS_2 modified SPCE help in differentiating peak current changes between smaller concentrations. This indicates that the SPCE shows better diffusion phenomena. The capacitive behavior for charge transfers due to the formation of a double-layer region helps in the better detection of diffusing Cu ion species.

IV. CONCLUSION

In this work, the systematic procedure for developing a thick film electrode via screen printing technique has been shown. The screen-printed carbon electrodes are modified with 2-dimensional MoS_2 nanoparticles dispersed in DMF solution. The electrochemical impedance studies carried out for the typical GCE-based electrochemical sensor and the modified screen-printed carbon electrodes allowed us to understand their capacitive and diffusion behavior. The SPCE-based sensors show better electrochemical performance than the GCE-based sensor. Whilst the better diffusion-controlled phenomena were observed in modified GCE, the capacitive behavior observed in SPCE helps to attain higher sensitivity for the detection of copper ions in water. The interference study shows that the presence of ferrous ions could affect the detection of copper. The observed detection range between 5 µM to 5 mM with a LOD of 5.43 µM, makes the presented sensor well-suited for the detection of copper ions in water resources. Further, the flexible form factor of the sensors and the low-cost fabrication make them an attractive alternative to the currently expensive, rigid sensor used for field testing.

ACKNOWLEDGEMENT

This work was started by R. Dahiya's Bendable Electronics and Sensing Technologies (BEST) Group when he was at University of Glasgow. The work got completed after he moved to Northeastern University, where his group is known as Bendable Electronics and Sustainable Technologies (BEST) Group.

REFERENCES

[1] L. Manjakkal, S. Mitra, Y. R. Petillot, J. Shutler, E. M. Scott, M. Willander, and R. Dahiya, "Connected sensors, innovative sensor deployment, and intelligent data analysis for online water quality monitoring," *IEEE Internet of Things J.,* vol. 8, no. 18, pp. 13805-13824, 2021.

[2] B. Bansod, T. Kumar, R. Thakur, S. Rana, and I. Singh, "A review on various electrochemical techniques for heavy metal ions detection with different sensing platforms," *Biosensors and Bioelectronics,* vol. 94, pp. 443-455, 2017.

[3] A. N. Parks, M. G. Cantwell, D. R. Katz, M. A. Cashman, T. P. Luxton, K. T. Ho, and R. M. Burgess, "Assessing the release of copper from nanocopper-treated and conventional copper-treated lumber into marine waters I: Concentrations and rates," *Environ Toxicol Chem,* vol. 37, no. 7, pp. 1956-1968, 2018.

[4] K. A. Kirk, and S. Andreescu, "Easy-to-use sensors for field monitoring of copper contamination in water and pesticide-sprayed plants," *Analytical chemistry,* vol. 91, no. 21, pp. 13892-13899, 2019.

[5] D. Maddipatla, T. S. Saeed, B. B. Narakathu, S. O. Obare, and M. Z. Atashbar, "Incorporating a novel hexaazatriphenylene derivative to a flexible screen-printed electrochemical sensor for copper ion detection in water samples," *IEEE Sensors J.,* vol. 20, no. 21, pp. 12582-12591, 2020.

[6] G. Polino, R. Abbel, S. Shanmugam, G. J. Bex, R. Hendriks, F. Brunetti, A. Di Carlo, R. Andriessen, and Y. Galagan, "A benchmark study of commercially available copper nanoparticle inks for application in organic electronic devices," *Organic electronics,* vol. 34, pp. 130-138, 2016.

[7] A. Ruiz, and K. L. Ogden, "Biotreatment of copper and isopropyl alcohol in waste from semiconductor manufacturing," *IEEE Trans. semicond. manufact.,* vol. 17, no. 4, pp. 538-543, 2004.

[8] C. A. Flemming, and J. T. Trevors, "Copper toxicity and chemistry in the environment: a review," *Water, Air, and Soil Pollution,* vol. 44, no. 1, pp. 143-158, 1989.

[9] T. Wen, F. Qu, N. B. Li, and H. Q. Luo, "A facile, sensitive, and rapid spectrophotometric method for copper (II) ion detection in aqueous media using polyethyleneimine," *Arabian J. Chemistry,* vol. 10, pp. S1680-S1685, 2017.

[10] J. R. Turnlund, "Copper nutriture, bioavailability, and the influence of dietary factors," *J. American Dietetic Association,* vol. 88, no. 3, pp. 303-308, 1988.

[11] B. R. Stern, "Essentiality and toxicity in copper health risk assessment: overview, update and regulatory considerations," *J. Toxicology and Environmental Health, Part A,* vol. 73, no. 2-3, pp. 114-127, 2010.

[12] G. J. Brewer, and V. Yuzbasiyan-Gurkan, "Wilson disease," *Medicine,* vol. 71, no. 3, pp. 139-164, 1992.

[13] L. Tang, X. Dai, X. Wen, D. Wu, and Q. Zhang, "A rhodamine–benzothiazole conjugated sensor for colorimetric, ratiometric and sequential recognition of copper (II) and sulfide in aqueous media," *Spectrochimica Acta Part A: Molecular and Biomolecular Spectroscopy,* vol. 139, pp. 329-334, 2015.

[14] R. Liu, Z. Chen, S. Wang, C. Qu, L. Chen, and Z. Wang, "Colorimetric sensing of copper (II) based on catalytic etching of gold nanoparticles," *Talanta,* vol. 112, pp. 37-42, 2013.

[15] A. Kindness, C. N. Sekaran, and J. Feldmann, "Two-dimensional mapping of copper and zinc in liver sections by laser ablation–inductively coupled plasma mass spectrometry," *Clinical chemistry,* vol. 49, no. 11, pp. 1916-1923, 2003.

[16] M. A. Levine, "Determining the provenance of native copper artifacts from northeastern North America: Evidence from instrumental neutron activation analysis," *Journal of Archaeological Science,* vol. 34, no. 4, pp. 572-587, 2007.

[17] G. K. Czamanske, E. Roedder, and F. C. Burns, "Neutron activation analysis of fluid inclusions for copper, manganese, and zinc," *Science,* vol. 140, no. 3565, pp. 401-403, 1963.

[18] M. Porento, V. Sutinen, T. Julku, and R. Oikari, "Detection of copper in water using on-line plasma-excited atomic absorption spectroscopy (AAS)," *Applied Spectroscopy,* vol. 65, no. 6, pp. 678-683, 2011.

[19] D. Citak, and M. Tuzen, "A novel preconcentration procedure using cloud point extraction for determination of lead, cobalt and copper in water and food samples using flame atomic absorption spectrometry," *Food and Chemical toxicology,* vol. 48, no. 5, pp. 1399-1404, 2010.

[20] B. Hołyńska, B. Ostachowicz, and D. Węgrzynek, "Simple method of determination of copper, mercury and lead in potable water with preliminary pre-concentration by total reflection X-ray fluorescence spectrometry," *Spectrochimica Acta Part B: Atomic Spectroscopy,* vol. 51, no. 7, pp. 769-773, 1996.

[21] J. Gao, J. Yin, Z. Tao, Y. Liu, X. Lin, J. Deng, and S. Wang, "An Ultrasensitive Fluorescence Sensor with Simple Operation for Cu2+ Specific Detection in Drinking Water," *ACS Omega,* vol. 3, no. 3, pp. 3045-3050, 2018.

[22] A. Beniwal, P. Ganguly, A. K. Aliyana, G. Khandelwal, and R. Dahiya, "Screen-printed graphene-carbon ink based disposable humidity sensor with wireless communication," *Sensors and Actuators B: Chemical*, vol. 374, pp. 132731, 2022.

[23] A. K. Aliyana, P. Ganguly, A. Beniwal, S. N. Kumar, and R. Dahiya, “Disposable pH Sensor on Paper Using Screen-Printed Graphene-Carbon Ink Modified Zinc Oxide Nanoparticles,” *IEEE Sensors J.,* 2022, doi: 10.1109/JSEN.2022.3206212.
[24] A. Vilouras, A. Christou, L. Manjakkal, and R. Dahiya, “Ultrathin ion-sensitive field-effect transistor chips with bending-induced performance enhancement,” *ACS Appl. Electronic Mater.,* vol. 2, no. 8, pp. 2601-2610, 2020.
[25] G. Khandelwal, and R. Dahiya, “Self-Powered Active Sensing based on Triboelectric Generator,” *Adv. Mater.*, pp. 2200724, 2022.
[26] Z. Zhao, C. Huang, Z. Huang, F. Lin, Q. He, D. Tao, N. Jaffrezic-Renault, and Z. Guo, “Advancements in electrochemical biosensing for respiratory virus detection: A review,” *TrAC Trends in Analytical Chemistry,* vol. 139, pp. 116253, 2021.
[27] S. Lakard, I.-A. Pavel, and B. Lakard, "Electrochemical Biosensing of Dopamine Neurotransmitter: A Review," *Biosensors,* 11, 2021.
[28] S. S. Low, D. Ji, W. S. Chai, J. Liu, K. S. Khoo, S. Salmanpour, F. Karimi, B. Deepanraj, and P. L. Show, "Recent Progress in Nanomaterials Modified Electrochemical Biosensors for the Detection of MicroRNA," *Micromachines,* 12, 2021.
[29] B. Viguier, K. Zór, E. Kasotakis, A. Mitraki, C. H. Clausen, W. E. Svendsen, and J. Castillo-León, “Development of an Electrochemical Metal-Ion Biosensor Using Self-Assembled Peptide Nanofibrils,” *ACS Applied Materials & Interfaces,* vol. 3, no. 5, pp. 1594-1600, 2011.
[30] B. S. Flavel, M. Nambiar, and J. G. Shapter, “Electrochemical Detection of Copper Using a Gly-Gly-His Modified Carbon Nanotube Biosensor,” *Silicon,* vol. 3, no. 4, pp. 163-171, 2011.
[31] M. Lin, X. Hu, Z. Ma, and L. Chen, “Functionalized polypyrrole nanotube arrays as electrochemical biosensor for the determination of copper ions,” *Analytica Chimica Acta,* vol. 746, pp. 63-69, 2012.
[32] A. Sinha, Dhanjai, B. Tan, Y. Huang, H. Zhao, X. Dang, J. Chen, and R. Jain, “MoS2 nanostructures for electrochemical sensing of multidisciplinary targets: A review,” *TrAC Trends in Analytical Chemistry,* vol. 102, pp. 75-90, 2018.
[33] N. Mphuthi, L. Sikhwivhilu, and S. S. Ray, "Functionalization of 2D MoS2 Nanosheets with Various Metal and Metal Oxide Nanostructures: Their Properties and Application in Electrochemical Sensors," *Biosensors,* 12, 2022.
[34] O. Samy, S. Zeng, M. D. Birowosuto, and A. El Moutaouakil, "A Review on MoS2 Properties, Synthesis, Sensing Applications and Challenges," *Crystals,* 11, 2021.
[35] T. Wang, K. Du, W. Liu, J. Zhang, and M. Li, “Electrochemical Sensors Based on Molybdenum Disulfide Nanomaterials,” *Electroanalysis,* vol. 27, no. 9, pp. 2091-2097, 2015.
[36] L. Manjakkal, D. Shakthivel, and R. Dahiya, “Flexible Printed Reference Electrodes for Electrochemical Applications,” *Adv. Mater. Techn.,* vol. 3, no. 12, pp. 1800252, 2018.
[37] K. Shrivas, A. Ghosale, P. K. Bajpai, T. Kant, K. Dewangan, and R. Shankar, “Advances in flexible electronics and electrochemical sensors using conducting nanomaterials: A review,” *Microchemical J.,* vol. 156, pp. 104944, 2020.
[38] M. Chakraborty, J. Kettle, and R. Dahiya, “Electronic waste reduction through devices and printed circuit boards designed for circularity,” *IEEE J. Flexible Electronics,* vol. 1, no. 1, pp. 4-23, 2022.
[39] M. Shojaei Baghini, A. Vilouras, M. Douthwaite, P. Georgiou, and R. Dahiya, “Ultra-thin ISFET-based sensing systems,” *Electrochemical Sc. Adv.*, pp. e2100202, 2021.
[40] D. K. Neethipathi, P. Ganguly, A. Beniwal, M. Scott, A. Bass, and R. Dahiya, "MoS 2 modified screen printed carbon electrode based flexible sensor for detection of Copper." IEEE Int. Conf. on Flexible, Printable Sensors and Systems (FLEPS), Vienna, Austria, 2022, pp. 1-4, doi: 10.1109/FLEPS53764.2022.9781564.
[41] S. B. Saseendran, A. Asha, and M. Jayaraj, "Hydrothermal synthesis of MoS2 for supercapacitive application." p. 070034, doi: 10.1063/5.0009010.
[42] L. Manjakkal, A. Vilouras, and R. Dahiya, “Screen Printed Thick Film Reference Electrodes for Electrochemical Sensing,” *IEEE Sensors J.,* vol. 18, no. 19, pp. 7779-7785, 2018.
[43] H. Adhikari, C. Ranaweera, R. Gupta, and S. Mishra, “Facile hydrothermal synthesis of molybdenum disulfide (MoS2) as advanced electrodes for super capacitors applications,” *MRS Adv.,* vol. 1, no. 45, pp. 3089-3097, 2016.
[44] X. Liu, Y. Yao, Y. Ying, and J. Ping, “Recent advances in nanomaterial-enabled screen-printed electrochemical sensors for heavy metal detection,” *TrAC Trends in Analytical Chemistry,* vol. 115, pp. 187-202, 2019.
[45] A. Ejaz, J. H. Han, and R. Dahiya, “Influence of solvent molecular geometry on the growth of nanostructures,” *J. colloid and interface science,* vol. 570, pp. 322-331, 2020.
[46] A. Pullanchiyodan, L. Manjakkal, and R. Dahiya, “Metal coated fabric based asymmetric supercapacitor for wearable applications,” *IEEE Sensors J.,* vol. 21, no. 23, pp. 26208-26214, 2021.
[47] A. Pullanchiyodan, L. Manjakkal, M. Ntagios, and R. Dahiya, “MnO x-electrodeposited fabric-based stretchable supercapacitors with intrinsic strain sensing,” *ACS Appl. Mater. & Interfaces,* vol. 13, no. 40, pp. 47581-47592, 2021.
[48] D. V. Thomaz, A. M. de Aguiar Filho, I. Y. L. De Macedo, E. S. B. Rodrigues, and E. D. S. Gil, “Predictive modelling to study the electrochemical behaviour of PdO, TiO2 and perovskite-type LaFeO3 modified carbon paste electrodes,” *Traektoriâ Nauki Path of Science,* vol. 5, no. 4, pp. 4001-4007, 2019.
[49] T. S. Mathis, N. Kurra, X. Wang, D. Pinto, P. Simon, and Y. Gogotsi, “Energy Storage Data Reporting in Perspective—Guidelines for Interpreting the Performance of Electrochemical Energy Storage Systems,” *Adv. Energy Mater.,* vol. 9, no. 39, pp. 1902007, 2019.

Deepan Kumar Neethipathi received his bachelor’s degree in Chemical engineering (B.Tech) from Anna university, India in 2017, and later, his master’s degree in Energy Science and Engineering (M.S) from Daegu Gyeongbuk Institute of Science and Technology, South Korea (DGIST) in 2020. Under the AQUASENSE project, He is working as a Marie Curie Early-Stage researcher at University of Glasgow since October 2020. His current research interest includes electrochemical sensors for water quality monitoring sensors and food quality-based application.

Ajay Beniwal received his B.Tech. and M.Tech. degree in Electronics and Communication Engineering from Kurukshetra University Kurukshetra, India, in 2013 and 2015, respectively, and a Ph.D. degree from the Department of Electronics and Communication Engineering, Indian Institute of Information Technology, Allahabad, Prayagraj, India in 2021. He is currently working as a Marie Curie Early-Stage Researcher with the Bendable Electronics and Sensing Technologies (BEST) Group, University of Glasgow, U.K. His current research interest includes material characterization and thin film technology, electronic sensor devices, and printed and flexible electronics, for healthcare and agriculture applications.

Adrian M. Bass is Senior Lecturer in University of Glasgow. He is a carbon cycle biogeochemist specialising in quantifying fluxes and controls in aquatic systems and as terrestrial aquatic interfaces. Dr Bass received undergraduate B.Sc in Marine Biology from the University of Wales, Swansea (1st class hon. 2004) and a Ph.D in Biogeochemistry from the University of Glasgow (2008). He completed 5-years post-doctoral research at James Cook University and Western Sydney University, Australia. Dr Bass has authored / co-authored >30 publications in academic literature and is investigator / co-investigator on >£15 million of active research grants.

Marian Scott is Professor of Environmental Statistics at University of Glasgow. Her research interests are in the application of statistical methods to environmental sciences. Projects include water and air quality, design of monitoring networks, the development of environmental indicators, and quantifying the state of the environment. She is additionally Vice-President (International) of the Royal Society of Edinburgh and a member of the Scottish Science Advisory Council. In 2005, Scott was elected a Fellow of the Royal Society of Edinburgh (FRSE), Scotland's national academy of science and letters. In the 2009 Queen's Birthday Honours, she was appointed an Officer of the Order of the British Empire (OBE) for services to social science. Professor Scott was awarded the Royal Statistical Society Barnett Award in 2019 for "her outstanding, pioneering research into the application of innovative statistical techniques to environmental issues."

Ravinder Dahiya (Fellow, IEEE) is Professor in ECE Department at Northeastern University, Boston, USA. He is the leader of Bendable Electronics and Sustainable Technologies (BEST) research group (*formerly*, Bendable Electronics and Sensing Technologies (BEST) group). His group conducts fundamental and applied research in flexible and printable electronics, tactile sensing, electronic skin, robotics, and wearable systems. He has authored or co-authored about 500 publications, books and submitted/granted patents and disclosures. He has led several international projects. He is President (2022-23) of the IEEE Sensors Council. He is the Founding Editor in Chief of IEEE JOURNAL ON FLEXIBLE ELECTRONICS (J-FLEX) and has served on the editorial boards of IEEE SENSORS JOURNAL (2012-2020) and IEEE TRANSACTIONS ON ROBOTICS (2012-2017). He was the Technical Program co-chair of IEEE Sensors 2017 and IEEE Sensors 2018 and has been General Chair/Co-Chair of several conferences including IEEE FLEPS (2019, 2020, 2021), which he founded in 2019, and IEEE Sensors 2023. He is recipient of EPSRC Fellowship, Marie Curie and Japanese Monbusho Fellowships. He has received several awards, including 2016 Microelectronic Engineering Young Investigator Award (Elsevier), 2016 Technical Achievement Award from the IEEE Sensors Council and 12 best paper awards as author/co-author in International Conferences and Journal.